

IMAGING WITH ELECTROMAGNETIC WAVES IN TERMINATING WAVEGUIDES

LILIANA BORCEA AND DINH-LIEM NGUYEN*

Abstract. We study an inverse scattering problem for Maxwell's equations in terminating waveguides, where localized reflectors are to be imaged using a remote array of sensors. The array probes the waveguide with waves and measures the scattered returns. The mathematical formulation of the inverse scattering problem is based on the electromagnetic Lippmann-Schwinger integral equation and an explicit calculation of the Green tensor. The image formation is carried with reverse time migration and with ℓ_1 optimization.

Key words. electromagnetic, terminating waveguide, inverse scattering.

1. Introduction. We consider an inverse scattering problem for Maxwell's equations in a waveguide which contains a few unknown reflectors. The setup is illustrated in Figure 1.1, where an array of sensors probes the waveguide with waves and records the returns over the duration of some time window. The inverse problem is to reconstruct the reflectors from these measurements.

To carry out explicit calculations we assume that the waveguide has a simple geometry, with rectangular cross-section $\Omega = (0, L_1) \times (0, L_2)$, and introduce the system of coordinates $\vec{x} = (\mathbf{x}, x_3)$, with $\mathbf{x} = (x_1, x_2) \in \Omega$ and $x_3 \leq 0$. The waveguide terminates at $x_3 = 0$ and we denote its domain by

$$W = (0, L_1) \times (0, L_2) \times (-\infty, 0),$$

with boundary ∂W . For convenience we model the boundaries as perfectly conducting, but other boundary conditions may be used.

The electric field $\vec{E}(\omega, \vec{x})$, decomposed over frequencies ω , satisfies the equation

$$\vec{\nabla} \times \vec{\nabla} \times \vec{E}(\omega, \vec{x}) - \omega^2 \mu_o \varepsilon(\omega, \vec{x}) \vec{E}(\omega, \vec{x}) = i\omega \mu_o \vec{J}(\omega, \mathbf{x}) \delta(x_3 + L), \quad \vec{x} \in W, \quad (1.1)$$

with boundary conditions

$$\vec{n}(\vec{x}) \times \vec{E}(\omega, \vec{x}) = 0 \quad \text{on } \partial W, \quad (1.2)$$

where $\vec{\nabla} \times$ is the curl operator in \mathbb{R}^3 and $\vec{n}(\vec{x})$ is the unit outer normal at ∂W . There is also a radiation condition at $x_3 \rightarrow -\infty$, which states that $\vec{E}(\omega, \vec{x})$ is bounded and outgoing. The current source density \vec{J} models the excitation from the array located at distance L from the terminating boundary at $x_3 = 0$.

The waveguide is filled with a linear and isotropic homogeneous medium with electric permittivity ε_o and magnetic permeability μ_o , and a few reflectors supported in the compact domain $D \subset W$, located between the array and the terminating boundary. The reflectors are modeled as linear and possibly anisotropic dielectrics with Hermitian, positive definite relative electric permittivity matrix $\varepsilon_r(\omega, \vec{x})$. The term $\varepsilon \vec{E}$ in (1.1) is the electric displacement, and ε is the electric permittivity tensor satisfying

$$\varepsilon(\omega, \vec{x}) = \varepsilon_o \left[1_D(\vec{x}) \left(\varepsilon_r(\omega, \vec{x}) - I \right) + I \right]. \quad (1.3)$$

Here I is the 3×3 identity matrix and $1_D(\vec{x})$ is the indicator function, equal to one for $\vec{x} \in D$ and zero otherwise.

*Department of Mathematics, University of Michigan, Ann Arbor, MI, 48109, USA; borcea@umich.edu and dlnghuyen@umich.edu

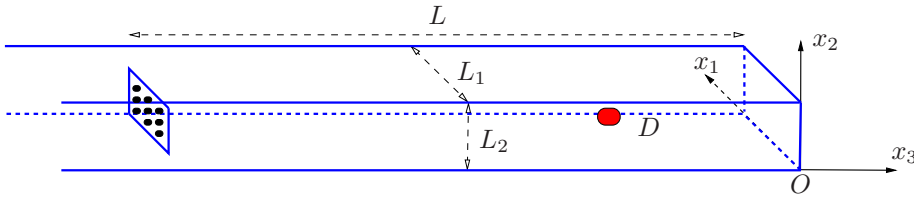


Figure 1.1: Schematic of the imaging setup in a terminating waveguide with rectangular cross-section. The unknown reflector is supported in D . The array of sensors is far away from it, at distance L from the terminating boundary.

The inverse problem is to reconstruct the perturbation $\varepsilon_r - I$ in (1.3), or at least its support D , from measurements of the electric field $\vec{E}(\omega, \vec{x})$ at points $\vec{x} = (\mathbf{x}, -L)$ in the array aperture A , a subset of Ω .

Inverse scattering and inverse source problems in waveguides have been considered in the past in various setups relevant to applications in ocean acoustics, non-destructive evaluation and imaging in tunnels. We refer to [2, 5–9, 19, 20, 23, 24] for mathematical studies of inverse scattering problems in acoustic and elastic waveguides with straight walls, and filled with homogeneous media. Random acoustic waveguides with finite cross-section are considered in [4, 11], and with unbounded cross-section, as encountered in ocean acoustics, in [3, 21]. Examples of inverse scattering problems in planar electromagnetic waveguides are in [13, 17, 22], where the problem is reduced to one for the scalar Helmholtz equation by considering a single type of waves, transverse electric or magnetic.

In this paper we give the mathematical formulation of the electromagnetic scattering problem in terminating waveguides and study with numerical simulations two imaging methods. The first is a reverse time migration approach, where the wave field measured at the array is time reversed and propagated to the imaging region using the electromagnetic Green’s tensor in the unperturbed waveguide. The second method uses ℓ_1 optimization, and is motivated by the assumption that the perturbation of the electric permittivity has small spatial support D .

The paper is organized as follows: We begin in section 2 with the formulation of the forward problem. We define the scattered electric field and show that it satisfies a Lipmann-Schwinger type equation. The solvability of this equation is analyzed using the Fredholm alternative. The data model used for inversion is given in section 3 and the imaging methods are formulated in section 4. The imaging results obtained with numerical simulations are in section 5. We end with a summary in section 6.

2. The scattering problem. In this section we formulate the scattering problem. We begin in section 2.1 with the expression of the electric field in the unperturbed (homogeneous) waveguide. Then we define in section 2.2 the scattered wave field at the unknown reflectors and derive the radiation condition at $x_3 \rightarrow -\infty$. We state the scattering problem as a Lippmann-Schwinger integral equation and prove its Fredholm property in section 2.3.

2.1. The homogeneous waveguide. In the absence of any reflector in the waveguide the electric field is denoted by \vec{E}^o , and solves the boundary value problem

$$\begin{aligned}\vec{\nabla} \times \vec{\nabla} \times \vec{E}^o(\vec{x}) - k^2 \vec{E}^o(\vec{x}) &= i\omega\mu_o \vec{J}(\vec{x})\delta(x_3 + L) \quad \vec{x} = (\vec{x}, x_3) \in W, \\ \vec{n}(\vec{x}) \times \vec{E}^o(\vec{x}) &= 0 \quad \vec{x} \in \partial W,\end{aligned}\tag{2.1}$$

where $k = \omega\sqrt{\varepsilon_o\mu_o}$ is the wavenumber. Obviously, \vec{E}^o and \vec{J} depend on the frequency ω , but since we consider a constant ω we simplify notation and drop it henceforth from the arguments of all fields. The expression of the electric field in infinite homogeneous waveguides is well known. See for example [12, chapter 8]. It is a superposition of a countable set of transverse electric and magnetic waves, called modes, which are either propagating away from the source or are decaying. In the terminating waveguide we have a similar mode decomposition of \vec{E}^o , as stated in Lemma 2.1, but there are both outgoing (forward propagating) and incoming (backward propagating) waves due to the reflection at the terminating boundary at $x_3 = 0$, and the evanescent waves may be growing or decaying away from the source, in the interval $x_3 \in (-L, 0)$.

The mode decomposition in Lemma 2.1 is obtained by expanding at each x_3 the field $\vec{E}^o(\vec{x})$ in the eigenfunctions $\vec{\Phi}_n^{(s)}(\vec{x})$ of the vectorial Laplacian

$$\begin{aligned}-\Delta \vec{\Phi}_n^{(s)}(\vec{x}) &= \lambda_n \vec{\Phi}_n^{(s)}(\vec{x}) \quad \vec{x} \in \Omega, \\ \vec{n}^\perp(\vec{x}) \cdot \vec{\Phi}_n^{(s)}(\vec{x}) &= \Phi_{n,3}(\vec{x}) = 0 \quad \vec{x} \in \partial\Omega, \\ \nabla \cdot \vec{\Phi}_n(\vec{x}) &= 0 \quad \vec{x} \in \partial\Omega.\end{aligned}\tag{2.2}$$

We refer to appendix A for a proof that $\{\vec{\Phi}_n^{(s)}(\vec{x})\}_{n \in \mathbb{N}_0^2, 1 \leq s \leq m_n}$ is an orthogonal basis of $(L^2(\Omega))^3$, and to [1, section 3] for an explanation of why the basis is useful for the analysis of electromagnetic waves in waveguides with perfectly conducting boundaries. In (2.2) the Laplacian Δ and divergence $\nabla \cdot$ are with respect to $\vec{x} \in \Omega$, \vec{n} is the outer normal at $\partial\Omega$, and \vec{n}^\perp is its rotation by 90 degrees, counter-clockwise. The vectors $\vec{\Phi}_n^{(s)} = (\Phi_n^{(s)}, \Phi_{n,3}^{(s)})$ are written in terms of their two dimensional projection $\Phi_n^{(s)}$ in the cross-section plane and the longitudinal part $\Phi_{n,3}^{(s)}$. The eigenvalues λ_n and eigenvectors $\vec{\Phi}_n^{(s)}$ are indexed by $n \in \mathbb{N}_0^2 = \{(n_1, n_2) : n_1^2 + n_2^2 \neq 0\}$ and the multiplicity index $s = 1, \dots, m_n$.

LEMMA 2.1. *The solution of (2.1) has the following mode decomposition*

$$\vec{E}^o(\vec{x}) = \sum_{n \in \mathbb{N}_0^2} \sum_{s=1}^{m_n} \vec{\Phi}_n^{(s)}(\vec{x}) \left(a_{o,n}^{+(s)} e^{i\beta_n x_3} + b_{o,n}^{-(s)} e^{-i\beta_n x_3} \right), \quad \text{for } x_3 \in (-L, 0), \tag{2.3}$$

and

$$\vec{E}^o(\vec{x}) = \sum_{n \in \mathbb{N}_0^2} \sum_{s=1}^{m_n} \vec{\Phi}_n^{(s)}(\vec{x}) b_{o,n}^{-(s)} e^{-i\beta_n x_3}, \quad \text{for } x_3 < -L, \tag{2.4}$$

where $a_{o,n}^\pm(s)$ and $b_{o,n}^\pm(s)$ are constant mode amplitudes determined by the current excitation $\vec{J}(\vec{x})$, and the superscripts \pm remind us that the field is evaluated in the forward direction (toward the terminating boundary) or away from it. The modes are waves with wavenumber

$$\beta_n = \begin{cases} \sqrt{k^2 - \lambda_n}, & k^2 \geq \lambda_n, \\ i\sqrt{\lambda_n - k^2}, & k^2 < \lambda_n. \end{cases} \tag{2.5}$$

For a finite number of indexes $n \in \mathbb{N}_0^2$ the wavenumbers β_n are real valued and the waves are propagating. The remaining infinitely many waves are evanescent.

Proof. Equations (2.3)-(2.4) are obtained by solving (2.1) with separation of variables. Since the eigenfunctions of the vectorial Laplacian in (2.2) form an orthogonal basis of $(L^2(\Omega))^3$, as shown in Appendix A, we can expand \vec{E}^o in this basis for each $x_3 \neq -L$. Equations (2.3)-(2.4) follow by substitution in (2.1) and straightforward calculation given in appendix B. The mode amplitudes are derived from jump conditions at the source coordinate $x_3 = -L$, reflection conditions at the terminating boundary at $x_3 = 0$, and the radiation condition at $x_3 \rightarrow -\infty$. The boundary conditions at $\partial\Omega$ are built into the expansion in the basis $\{\vec{\Phi}_n^{(s)}\}$. Note that in the interval $x_3 \in (-L, 0)$ between the source and the terminating boundary there are both forward and backward propagating waves and decaying and growing evanescent waves. On the other side of the source, for $x_3 < -L$, the propagating waves are outgoing and the evanescent waves are decaying, as imposed by the radiation condition. \square

The simple geometry of the waveguide, with rectangular cross-section, allows us to write explicitly the mode decomposition in (2.3)–(2.4). The eigenvalues are

$$\lambda_n = \left(\frac{\pi n_1}{L_1}\right)^2 + \left(\frac{\pi n_2}{L_2}\right)^2, \quad n = (n_1, n_2) \in \mathbb{N}_o^2, \quad (2.6)$$

and by assuming that $(L_1/L_2)^2$ is not a rational number, we ensure that $\lambda_n \neq \lambda_{n'}$ if $n = (n_1, n_2) \neq n' = (n'_1, n'_2)$. This limits the multiplicity m_n of the eigenvalues to

$$m_n = \begin{cases} 1 & \text{if } n_1 n_2 = 0, \\ 3 & \text{otherwise.} \end{cases} \quad (2.7)$$

For the index pairs satisfying $n_1 n_2 = 0$, the eigenvalues are simple, with eigenvectors

$$\vec{\Phi}_n^{(1)}(\mathbf{x}) = \delta_{n_2 0} \begin{pmatrix} 0 \\ \sin\left(\frac{\pi n_1 x_1}{L_1}\right) \\ 0 \end{pmatrix} + \delta_{n_1 0} \begin{pmatrix} \sin\left(\frac{\pi n_2 x_2}{L_2}\right) \\ 0 \\ 0 \end{pmatrix}, \quad (2.8)$$

satisfying the divergence free condition $\vec{\nabla} \cdot \vec{\Phi}^{(1)}(\mathbf{x}) = 0$. Otherwise, there is triple multiplicity of the eigenvalues, and the eigenvectors are given by

$$\vec{\Phi}_n^{(1)}(\mathbf{x}) = \begin{pmatrix} \frac{\pi n_2}{L_2} \cos\left(\frac{\pi n_1 x_1}{L_1}\right) \sin\left(\frac{\pi n_2 x_2}{L_2}\right) \\ -\frac{\pi n_1}{L_1} \sin\left(\frac{\pi n_1 x_1}{L_1}\right) \cos\left(\frac{\pi n_2 x_2}{L_2}\right) \\ 0 \end{pmatrix}, \quad (2.9)$$

$$\vec{\Phi}_n^{(2)}(\mathbf{x}) = \begin{pmatrix} \frac{\pi n_1}{L_1} \cos\left(\frac{\pi n_1 x_1}{L_1}\right) \sin\left(\frac{\pi n_2 x_2}{L_2}\right) \\ \frac{\pi n_2}{L_2} \sin\left(\frac{\pi n_1 x_1}{L_1}\right) \cos\left(\frac{\pi n_2 x_2}{L_2}\right) \\ 0 \end{pmatrix}, \quad (2.10)$$

which are vectors in the cross-range plane, satisfying the divergence free condition $\vec{\nabla} \cdot \vec{\Phi}^{(1)}(\mathbf{x}) = 0$ and the curl free condition $\vec{\nabla} \times \vec{\Phi}^{(2)}(\mathbf{x}) = 0$, and

$$\vec{\Phi}_n^{(3)}(\mathbf{x}) = \begin{pmatrix} 0 \\ 0 \\ \sin\left(\frac{\pi n_1 x_1}{L_1}\right) \sin\left(\frac{\pi n_2 x_2}{L_2}\right) \end{pmatrix}, \quad (2.11)$$

which is in the longitudinal direction.

Equations (2.3)–(2.4) take the explicit form

$$\begin{aligned}\vec{E}^o(\vec{x}) = \sum_{n \in \mathbb{N}_0^2} \sum_{s=1}^{m_n} & \left[\delta_{s1} \vec{\Phi}_n^{(1)}(\mathbf{x}) (a_{o,n}^{+(1)} e^{i\beta_n x_3} + b_{o,n}^{+(1)} e^{-i\beta_n x_3}) \right. \\ & + \left(\delta_{s2} \vec{\Phi}_n^{(2)}(\mathbf{x}) - \frac{i\lambda_n}{\beta_n} \delta_{s3} \vec{\Phi}_n^{(3)}(\mathbf{x}) \right) a_{o,n}^{+(2)} e^{i\beta_n x_3} \\ & \left. + \left(\delta_{s2} \vec{\Phi}_n^{(2)}(\mathbf{x}) + \frac{i\lambda_n}{\beta_n} \delta_{s3} \vec{\Phi}_n^{(3)}(\mathbf{x}) \right) b_{o,n}^{+(2)} e^{-i\beta_n x_3} \right], \quad \text{for } x_3 > -L,\end{aligned}\tag{2.12}$$

and

$$\begin{aligned}\vec{E}^o(\vec{x}) = \sum_{n \in \mathbb{N}_0^2} \sum_{s=1}^{m_n} & \left[\delta_{s1} \vec{\Phi}_n^{(1)}(\mathbf{x}) b_{o,n}^{-(1)} e^{-i\beta_n x_3} + \right. \\ & \left. \left(\delta_{s2} \vec{\Phi}_n^{(2)}(\mathbf{x}) + \frac{i\lambda_n}{\beta_n} \delta_{s3} \vec{\Phi}_n^{(3)}(\mathbf{x}) \right) b_{o,n}^{-(2)} e^{-i\beta_n x_3} \right], \quad \text{for } x_3 < -L.\end{aligned}\tag{2.13}$$

The field \vec{E}^o is a superposition of transverse electric waves with amplitudes $a_{n,o}^{+(1)}$ and $b_{n,o}^{\pm(1)}$, and transverse magnetic waves with amplitudes $a_{n,o}^{+(2)}$ and $b_{n,o}^{\pm(2)}$. The name transverse electric refers to the fact that the third component of $\vec{\Phi}_n^{(1)}(\mathbf{x})$, corresponding to the longitudinal electric field, equals zero. Similarly, the name transverse magnetic refers to the fact that

$$\vec{e}_3 \cdot \vec{\nabla} \times \left(\vec{\Phi}_n^{(2)}(\mathbf{x}) \pm \frac{i\lambda_n}{\beta_n} \vec{\Phi}_n^{(3)}(\mathbf{x}) \right) = \vec{e}_3 \cdot \vec{\nabla} \times \vec{\Phi}_n^{(2)}(\mathbf{x}) = 0,$$

and thus the longitudinal magnetic field is zero by Faraday's law.

The transverse electric mode amplitudes are given by

$$a_{o,n}^{+(1)} = -\frac{\omega\mu_o \langle \vec{\Phi}_n^{(1)}, \vec{\mathbf{J}} \rangle}{2\beta_n \|\vec{\Phi}_n^{(1)}\|^2} e^{i\beta_n L}, \quad b_{o,n}^{+(1)} = \frac{\omega\mu_o \langle \vec{\Phi}_n^{(1)}, \vec{\mathbf{J}} \rangle}{2\beta_n \|\vec{\Phi}_n^{(1)}\|^2} e^{i\beta_n L}, \tag{2.14}$$

for $x_3 \in (-L, 0)$ and by

$$b_{o,n}^{-(1)} = \frac{\omega\mu_o \langle \vec{\Phi}_n^{(1)}, \vec{\mathbf{J}} \rangle}{2\beta_n \|\vec{\Phi}_n^{(1)}\|^2} [e^{i\beta_n L} - e^{-i\beta_n L}], \tag{2.15}$$

for $x_3 < -L$. Here $\langle \cdot, \cdot \rangle$ denotes the inner product in $(L^2(\Omega))^3$ and $\|\cdot\|$ is the induced norm. The transverse magnetic mode amplitudes are

$$\begin{aligned}a_{o,n}^{+(2)} &= \left[-\frac{\omega\mu_o\beta_n}{2k^2} \frac{\langle \vec{\Phi}_n^{(2)}, \vec{\mathbf{J}} \rangle}{\|\vec{\Phi}_n^{(2)}\|^2} - \frac{i\omega\mu_o}{2\lambda_n} \frac{\langle \vec{\Phi}_n^{(3)}, \vec{\mathbf{J}} \rangle}{\|\vec{\Phi}_n^{(3)}\|^2} \right] e^{i\beta_n L}, \\ b_{o,n}^{+(2)} &= \left[\frac{\omega\mu_o\beta_n}{2k^2} \frac{\langle \vec{\Phi}_n^{(2)}, \vec{\mathbf{J}} \rangle}{\|\vec{\Phi}_n^{(2)}\|^2} + \frac{i\omega\mu_o}{2\lambda_n} \frac{\langle \vec{\Phi}_n^{(3)}, \vec{\mathbf{J}} \rangle}{\|\vec{\Phi}_n^{(3)}\|^2} \right] e^{i\beta_n L},\end{aligned}\tag{2.16}$$

for $x_3 \in (-L, 0)$ and

$$b_{o,n}^{-(2)} = \frac{\omega\mu_o\beta_n}{2k^2} \frac{\langle \vec{\Phi}_n^{(2)}, \vec{\mathbf{J}} \rangle}{\|\vec{\Phi}_n^{(2)}\|^2} [e^{i\beta_n L} - e^{-i\beta_n L}] + \frac{i\omega\mu_o}{2\lambda_n} \frac{\langle \vec{\Phi}_n^{(3)}, \vec{\mathbf{J}} \rangle}{\|\vec{\Phi}_n^{(3)}\|^2} [e^{i\beta_n L} + e^{-i\beta_n L}], \tag{2.17}$$

for $x_3 < -L$.

2.2. The scattered field and radiation condition. The scattered field due to the reflectors supported in $D \subset W$ is defined by

$$\vec{E}^{sc}(\vec{x}) = \vec{E}(\vec{x}) - \vec{E}^o(\vec{x}), \quad (2.18)$$

where $\vec{E}(\vec{x})$ is the solution of equation (1.1), with the electric permittivity tensor (1.3). Explicitly, \vec{E}^{sc} satisfies

$$\begin{aligned} \vec{\nabla} \times \vec{\nabla} \times \vec{E}^{sc}(\vec{x}) - k^2 \vec{E}^{sc}(\vec{x}) &= k^2 V(\vec{x}) \vec{E}(\vec{x}) & \vec{x} \in W, \\ \vec{n}(\vec{x}) \times \vec{E}^{sc}(\vec{x}) &= 0 & \vec{x} \in \partial W, \end{aligned} \quad (2.19)$$

where

$$V(\vec{x}) = \frac{\varepsilon(\vec{x})}{\varepsilon_o} - I = 1_D(\vec{x})(\varepsilon_r(\vec{x}) - I) \quad (2.20)$$

is the scattering potential. The radiation condition, which states that the scattered field is bounded and outgoing away from the reflectors, takes the form

$$\begin{aligned} \vec{E}^{sc}(\vec{x}) &= \sum_{n \in \mathbb{N}_0^2} \sum_{s=1}^{m_n} \left[\delta_{s1} \vec{\Phi}_n^{(1)}(\vec{x}) b_n^{-(1)} e^{-i\beta_n x_3} \right. \\ &\quad \left. + \left(\delta_{s2} \vec{\Phi}_n^{(2)}(\vec{x}) + \frac{i\lambda_n}{\beta_n} \delta_{s3} \vec{\Phi}_n^{(3)}(\vec{x}) \right) b_n^{-(2)} e^{-i\beta_n x_3} \right], \end{aligned} \quad (2.21)$$

for locations $\vec{x} = (\vec{x}, x_3) \in W$ satisfying $x_3 < \inf\{x_3 : \vec{x} = (x_1, x_2, x_3) \in D\}$. Note the similarity of (2.21) with (2.13), the expression of the reference field $\vec{E}^{(o)}$ on the left of the source. The mode amplitudes $b_n^{-(1)}$ and $b_n^{-(2)}$ contain the information about the reflectors supported in D and their expression follows from the calculations in the next section.

2.3. Solvability of the forward problem. Here we study the solvability of the forward scattering problem (2.19)–(2.21). We begin with the derivation of the Green's tensor $\mathbb{G}(\vec{x}, \vec{y})$ and then restate the scattering problem as an electromagnetic Lippmann-Schwinger equation, for which we can prove the Fredholm property. The discussion assumes that the domain D that supports the reflectors does not touch the boundary, and that the scattering potential V is bounded, entrywise.

The Green's tensor $\mathbb{G}(\vec{x}, \vec{y}) \in \mathbb{C}^{3 \times 3}$ satisfies

$$\begin{aligned} \vec{\nabla} \times \vec{\nabla} \times \mathbb{G}(\vec{x}, \vec{y}) - k^2 \mathbb{G}(\vec{x}, \vec{y}) &= -\delta(\vec{x} - \vec{y}) I & \vec{x} \in W, \\ \vec{n}(\vec{x}) \times \mathbb{G}(\vec{x}, \vec{y}) &= 0 & \vec{x} \in \partial W, \end{aligned} \quad (2.22)$$

where we recall that I is the 3×3 identity matrix, and the curl is taken columnwise. In addition, each column of $\mathbb{G}(\vec{x}, \vec{y})$ satisfies a radiation condition similar to (2.21) for $x_3 < y_3$, which says that the Green's function is bounded and outgoing. The expression of \mathbb{G} is given in the next lemma, proved in appendix C.

LEMMA 2.2. *Let $\vec{x} \neq \vec{y}$ and $\vec{x}, \vec{y} \in W$. The Green's tensor $\mathbb{G}(\cdot, \vec{y})$ is given by*

$$\mathbb{G}(\vec{x}, \vec{y}) = (\vec{G}_1, \vec{G}_2, \vec{G}_3)(\vec{x}, \vec{y}) + \frac{1}{k^2} \vec{\nabla} \vec{\nabla} \cdot (\vec{G}_1, \vec{G}_2, \vec{G}_3)(\vec{x}, \vec{y}), \quad (2.23)$$

with divergence taken columnwise. The vectors \vec{G}_j with $j = 1, \dots, 3$ are defined by

$$\vec{G}_j(\vec{x}, \vec{y}) = \sum_{n \in \mathbb{N}_0^2} \sum_{s=1}^{m_n} \frac{\vec{e}_j \cdot \vec{\Phi}_n^{(s)}(\vec{y})}{\|\vec{\Phi}_n^{(s)}\|^2} [e^{i\beta_n|x_3-y_3|} + (2\delta_{s3} - 1)e^{-i\beta_n(x_3+y_3)}] \frac{\vec{\Phi}_n^{(s)}(\vec{x})}{2i\beta_n}. \quad (2.24)$$

They satisfy equations

$$\begin{aligned} \Delta \vec{G}_j(\vec{x}, \vec{y}) + k^2 \vec{G}_j(\vec{x}, \vec{y}) &= \delta(\vec{x} - \vec{y}) \vec{e}_j \quad \vec{x} \in W, \\ \vec{n}(\vec{x}) \times \left[k^2 \vec{G}_j(\vec{x}, \vec{y}) + \vec{\nabla} \vec{\nabla} \cdot \vec{G}_j(\vec{x}, \vec{y}) \right] &= 0 \quad \vec{x} \in \partial W, \end{aligned} \quad (2.25)$$

and a radiation condition similar to (2.21) for $x_3 < y_3$, which says that the components of \vec{G}_j are outgoing or decaying waves.

To state the scattering problem (2.19) as a Lippmann-Schwinger equation, we follow the approach in [15]. For a finite $\bar{L} \geq L$, we define the truncated waveguide

$$W_{\bar{L}} = (0, L_1) \times (0, L_2) \times (-\bar{L}, 0) \subset W,$$

and introduce the space

$$H(\text{curl}, W_{\bar{L}}) := \left\{ \vec{u} \in (L^2(W_{\bar{L}}))^3 : \vec{\nabla} \times \vec{u} \in (L^2(W_{\bar{L}}))^3 \right\},$$

equipped with the inner product

$$(\vec{u}, \vec{v})_{\text{curl}} = \int_{W_{\bar{L}}} d\vec{x} \left[\vec{u}(\vec{x}) \cdot \overline{\vec{v}(\vec{x})} + \vec{\nabla} \times \vec{u}(\vec{x}) \cdot \vec{\nabla} \times \overline{\vec{u}(\vec{x})} \right],$$

where the bar denotes complex conjugate. The induced norm is $\|\vec{u}\|_{\text{curl}} = \sqrt{(\vec{u}, \vec{u})_{\text{curl}}}$.

From [15] we know that $\mathcal{M} : (L^2(D))^3 \rightarrow H(\text{curl}, W_{\bar{L}})$ defined by

$$\mathcal{M}(\vec{u})(\vec{x}) = (k^2 + \vec{\nabla} \vec{\nabla} \cdot) \int_D \frac{e^{ik|\vec{x}-\vec{y}|}}{4\pi|\vec{x}-\vec{y}|} \vec{u}(\vec{y}) d\vec{y},$$

is a linear bounded mapping. Moreover, $\vec{v} = \mathcal{M}(\vec{u})$ is the unique radiating variational solution of $\vec{\nabla} \times \vec{\nabla} \times \vec{v} - k^2 \vec{v} = k^2 \vec{u}$, meaning that

$$\int_{W_{\bar{L}}} \left(\vec{\nabla} \times \vec{v} \cdot \vec{\nabla} \times \overline{\vec{\varphi}} - k^2 \vec{v} \cdot \overline{\vec{\varphi}} \right) d\vec{x} = k^2 \int_D \vec{g} \cdot \overline{\vec{\varphi}} d\vec{x} \quad (2.26)$$

for all $\vec{\varphi} \in H(\text{curl}, W_{\bar{L}})$, with compact support in $W_{\bar{L}}$. This result can be extended to our problem because the difference of Green's functions $\vec{G}_j(\vec{x}, \vec{y}) - \frac{e^{ik|\vec{x}-\vec{y}|}}{4\pi|\vec{x}-\vec{y}|} \vec{e}_j$ is analytic and satisfies

$$(\Delta + k^2) \left(\vec{G}_j(\vec{x}, \vec{y}) - \frac{e^{ik|\vec{x}-\vec{y}|}}{4\pi|\vec{x}-\vec{y}|} \vec{e}_j \right) = 0.$$

Thus, the mapping $\mathcal{L} : (L^2(D))^3 \rightarrow H(\text{curl}, W_{\bar{L}})$ defined by

$$\mathcal{L}(\vec{u}) = (k^2 + \vec{\nabla} \vec{\nabla} \cdot) \int_D (\vec{G}_1, \vec{G}_2, \vec{G}_3)(\cdot, \vec{y}) \vec{u}(\vec{y}) d\vec{y}, \quad (2.27)$$

is linear and bounded, and $\vec{v} = \mathcal{L}(\vec{u})$ is the radiating variational solution of the equation $\vec{\nabla} \times \vec{\nabla} \times \vec{v} - k^2 \vec{v} = k^2 \vec{u}$ in the waveguide. We are interested in $\vec{u} = V\vec{E}$, so that $\mathcal{L}(V\vec{E})$ satisfies the partial differential equation (2.19). To show that this is \vec{E}^{sc} it remains to check that $\mathcal{L}(V\vec{E})$ satisfies the perfectly conducting boundary conditions. This follows from the boundary conditions in (2.25), because D does not touch the boundary, so we can write

$$\vec{n}(\vec{x}) \times \mathcal{L}(\vec{u}) = \int_D \vec{n}(\vec{x}) \times (k^2 + \vec{\nabla} \vec{\nabla} \cdot) (\vec{G}_1, \vec{G}_2, \vec{G}_3)(\cdot, \vec{y}) \vec{u}(\vec{y}) d\vec{y} = 0, \quad \vec{x} \in \partial W.$$

We have now shown that $\vec{E}^{sc}(\vec{x}) = \mathcal{L}(V\vec{E})$, or equivalently, that it solves the Lippmann-Schwinger equation

$$\vec{E}^{sc}(\vec{x}) = (k^2 + \vec{\nabla} \vec{\nabla} \cdot) \int_D (\vec{G}_1, \vec{G}_2, \vec{G}_3)(\cdot, \vec{y}) V(\vec{y}) \vec{E}(\vec{y}) d\vec{y}. \quad (2.28)$$

The next Theorem proves a Gårding inequality from which we can conclude the Fredholm property.

THEOREM 2.3. *There exists a compact operator $\mathcal{K} : H(\text{curl}, W_L) \rightarrow H(\text{curl}, W_L)$ and a positive constant C such that*

$$\text{Re} \left(\vec{u} - \mathcal{L}(V\vec{u}) + \mathcal{K} \vec{u}, \vec{u} \right)_{\text{curl}} \geq C \|\vec{u}\|_{\text{curl}}^2, \quad \forall \vec{u} \in H(\text{curl}, W_L). \quad (2.29)$$

Therefore, $I - \mathcal{L}(V\cdot)$ is a Fredholm operator.

Proof. Let us define an auxilliary operator $\mathcal{L}_o : (L^2(D))^3 \rightarrow H(\text{curl}, W_L)$,

$$\mathcal{L}_o(\vec{u}) = (-1 + \vec{\nabla} \vec{\nabla} \cdot) \int_D (\vec{\mathcal{G}}_1, \vec{\mathcal{G}}_2, \vec{\mathcal{G}}_3)(\cdot, \vec{y}) \vec{u}(\vec{y}) d\vec{y}, \quad (2.30)$$

where $\vec{\mathcal{G}}_j$ solve

$$\Delta \vec{\mathcal{G}}_j(\vec{x}, \vec{y}) - \vec{\mathcal{G}}_j(\vec{x}, \vec{y}) = \delta(\vec{x} - \vec{y}) \vec{e}_j, \quad \vec{x} \in W_L. \quad (2.31)$$

These are like the partial differential equations in (2.25), with k replaced by the imaginary number i . From the analysis in [15], which applies to imaginary wavenumbers like i , we obtain that \mathcal{L}_o is a bounded linear operator and $\vec{u} = \mathcal{L}_o(\vec{f})$ is the weak solution of $\vec{\nabla} \times \vec{\nabla} \times \vec{u} + \vec{u} = -\vec{f}$. Explicitly, we have for all $\vec{\varphi} \in H(\text{curl}, W_L)$,

$$\begin{aligned} \left(\mathcal{L}_o(\vec{f}), \vec{\varphi} \right)_{\text{curl}} &= \int_{W_L} d\vec{x} \left[\vec{\nabla} \times \mathcal{L}_o(\vec{f}) \cdot \vec{\nabla} \times \vec{\varphi} + \mathcal{L}_o(\vec{f}) \cdot \vec{\varphi} \right] \\ &= - \int_D d\vec{x} \vec{f} \cdot \vec{\varphi} - \int_{\partial W_L} ds \left[\vec{n} \times \vec{\nabla} \times \mathcal{L}_o(\vec{f}) \right] \cdot \left[(\vec{n} \times \vec{\varphi}) \times \vec{n} \right], \end{aligned} \quad (2.32)$$

where we used the integration by parts result in [18, Theorem 3.31].

Using this auxiliary operator we write

$$\begin{aligned} \left(\vec{u} - \mathcal{L}(V\vec{u}), \vec{u} \right)_{\text{curl}} &= \left(\vec{u} - \mathcal{L}_o(V\vec{u}), \vec{u} \right)_{\text{curl}} - \left((\mathcal{L} - \mathcal{L}_o)(V\vec{u}), \vec{u} \right)_{\text{curl}} \\ &= \|\vec{u}\|_{\text{curl}}^2 - \left(\mathcal{L}_o(V\vec{u}), \vec{u} \right)_{\text{curl}} - \left((\mathcal{L} - \mathcal{L}_o)(V\vec{u}), \vec{u} \right)_{\text{curl}}, \end{aligned}$$

and from (2.32) with $\vec{f} = V\vec{u}$ and $\vec{\varphi} = \vec{u}$, we get

$$\begin{aligned} \left(\vec{u} - \mathcal{L}(V\vec{u}), \vec{u} \right)_{\text{curl}} &= \|\vec{u}\|_{\text{curl}}^2 + \int_D d\vec{x} (\varepsilon_r(\vec{x}) - I) \vec{u} \cdot \vec{u} \\ &+ \int_{\partial W_L} ds \left[\vec{n} \times \vec{\nabla} \times \mathcal{L}_o(V\vec{u}) \right] \cdot \left[(\vec{n} \times \vec{u}) \times \vec{n} \right] - \left((\mathcal{L} - \mathcal{L}_o)(V\vec{u}), \vec{u} \right)_{\text{curl}}. \end{aligned}$$

Here we used the expression (2.20) of V . Because ε_r is positive definite by assumption, we conclude that there exists a positive constant C such that

$$\|\vec{u}\|_{\text{curl}}^2 + \int_D d\vec{x} (\varepsilon_r(\vec{x}) - I) \vec{u} \cdot \vec{u} \geq C \|\vec{u}\|_{\text{curl}}^2, \quad \forall \vec{u} \in H(\text{curl}, W_L).$$

Substituting in the equation above and introducing the linear operators \mathcal{K}_1 and \mathcal{K}_2 from $H(\text{curl}, W_L)$ to $H(\text{curl}, W_L)$, defined by

$$\mathcal{K}_1(\vec{u}) = (\mathcal{L} - \mathcal{L}_o)(\vec{u}), \quad (2.33)$$

$$\mathcal{K}_2(\vec{u}) = - \int_{\partial W_L} ds \left[\vec{n} \times \vec{\nabla} \times \mathcal{L}_o(V\vec{u}) \right] \cdot \left[(\vec{n} \times \vec{u}) \times \vec{n} \right], \quad (2.34)$$

we obtain

$$\text{Re} \left(\vec{u} - \mathcal{L}(V\vec{u}) + \mathcal{K}_1(\vec{u}) + \mathcal{K}_2(\vec{u}), \vec{u} \right)_{\text{curl}} \geq C \|\vec{u}\|_{\text{curl}}^2, \quad \forall \vec{u} \in H(\text{curl}, W_L). \quad (2.35)$$

Result (2.28) follows once we show that \mathcal{K}_1 and \mathcal{K}_2 are compact operators.

Since the differences $\vec{G}_j(\vec{x}, \vec{y}) - \frac{e^{ik|\vec{x}-\vec{y}|}}{4\pi|\vec{x}-\vec{y}|} \vec{e}_j$ and $\vec{\mathcal{G}}_j(\vec{x}, \vec{y}) - \frac{e^{-|\vec{x}-\vec{y}|}}{4\pi|\vec{x}-\vec{y}|} \vec{e}_j$ are analytic, we conclude that the singularity of the kernel in $\mathcal{L} - \mathcal{L}_o$ is as strong as that of $\left[\frac{e^{ik|\vec{x}-\vec{y}|}}{4\pi|\vec{x}-\vec{y}|} - \frac{e^{-|\vec{x}-\vec{y}|}}{4\pi|\vec{x}-\vec{y}|} \right] I$. Thus, we can use the results in [15] to conclude that \mathcal{K}_1 is a compact operator.

To prove that \mathcal{K}_2 is compact, let us consider a neighborhood Γ of the boundary ∂W_L , such that $\Gamma \subset W_L$ and Γ does not intersect the support D of the scattering potential. We define the operator \mathcal{T} from $(L^2(D))^3$ to $(H^s(\Gamma))^3$, with $s > 1$, by restricting $\vec{\nabla} \times \mathcal{L}_o(\vec{f})$ to Γ , for all $\vec{f} \in (L^2(D))^3$,

$$\mathcal{T}(\vec{f}) = - \int_D d\vec{y} \nabla \times \left(\vec{\mathcal{G}}_1, \vec{\mathcal{G}}_2, \vec{\mathcal{G}}_3 \right) (\cdot, \vec{y}) \vec{f}(\vec{y}), \quad \text{in } \Gamma. \quad (2.36)$$

This operator is compact because its kernel is an analytic function on $\Gamma \times D$. Define also the trace space

$$H_{\text{div}}^{-1/2}(\partial W_L) = \left\{ \vec{f} \in \left(H^{-1/2}(\partial W_L) \right)^3 : \exists \vec{u} \in H(\text{curl}, W_L) \text{ satisfying } \vec{n} \times \vec{u}|_{\partial W_L} = \vec{f} \right\},$$

with norm

$$\|\vec{f}\|_{H_{\text{div}}^{-1/2}(\partial W_L)} = \inf_{\vec{u} \in H(\text{curl}, W_L), \vec{n} \times \vec{u}|_{\partial W_L} = \vec{f}} \|\vec{u}\|_{\text{curl}}.$$

It is shown in [18, Section 3.5] that $H_{\text{div}}^{-1/2}(\partial W_L)$ is a Banach space. Due to the compactness of \mathcal{T} , the mapping $\vec{u} \rightarrow \vec{n} \times \mathcal{T}(V\vec{u})|_{\partial W_L}$ is a compact operator from $H(\text{curl}, W_L)$ to $H_{\text{div}}^{-1/2}(\partial W_L)$. Note that the mapping $\vec{u} \rightarrow V\vec{u}$ is bounded from $H(\text{curl}, W_L)$ to $(L^2(D))^3$ and $\mathcal{T}(\vec{u}) \rightarrow \vec{n} \times \mathcal{T}(\vec{u})|_{\partial W_L}$ is bounded from $(H^s(D))^3$ to

$H_{\text{div}}^{-1/2}(\partial W_{\bar{L}})$. We also have from [18, Section 3.5] that $\vec{u} \rightarrow (\vec{n} \times \vec{u}|_{\partial W_{\bar{L}}}) \times \vec{n}$ is a linear bounded mapping from $H(\text{curl}, W_{\bar{L}})$ to $H_{\text{curl}}^{-1/2}(\partial W_{\bar{L}})$, the dual space of $H_{\text{div}}^{-1/2}(\partial W_{\bar{L}})$.

To show that \mathcal{K}_2 is compact, let $\{\vec{u}_j\}$ be a sequence in $H(\text{curl}, W_{\bar{L}})$ that converges weakly to 0, and prove that $\{\mathcal{K}_2(\vec{u}_j)\}$ converges strongly to 0 in $H(\text{curl}, W_{\bar{L}})$. Indeed we have

$$\begin{aligned} \|\mathcal{K}_2(\vec{u}_j)\|_{\text{curl}} &= \sup_{\vec{v} \in H(\text{curl}, W_{\bar{L}}) \setminus \{0\}} \frac{|(\mathcal{K}_2(\vec{u}_j), \vec{v})_{\text{curl}}|}{\|\vec{v}\|_{\text{curl}}} \\ &\leq \sup_{\vec{v} \in H(\text{curl}, W_{\bar{L}}) \setminus \{0\}} \frac{\|\vec{n} \times \vec{\nabla} \times \mathcal{L}_o(V\vec{u}_j)\|_{H_{\text{div}}^{-1/2}(\partial W_{\bar{L}})} \|\vec{n} \times \vec{v} \times \vec{n}\|_{H_{\text{curl}}^{-1/2}(\partial W_{\bar{L}})}}{\|\vec{v}\|_{\text{curl}}} \\ &\leq C \|\vec{n} \times \vec{\nabla} \times \mathcal{L}_o(V\vec{u}_j)\|_{H_{\text{div}}^{-1/2}(\partial W_{\bar{L}})} \\ &= C \|\vec{n} \times \mathcal{T}(V\vec{u}_j)\|_{H_{\text{div}}^{-1/2}(\partial W_{\bar{L}})} \\ &\rightarrow 0, \quad \text{as } j \rightarrow \infty. \end{aligned}$$

where the first line is a definition, the second line follows by duality, the third line is due to the boundedness of the mapping $\vec{v} \rightarrow \vec{n} \times \vec{v} \times \vec{n}$ and the fourth line is by the definition of \mathcal{T} . The convergence to zero is by the compactness of the mapping $\vec{u} \rightarrow \vec{n} \times \mathcal{T}(V\vec{u})|_{\partial W_{\bar{L}}}$.

We have now proved the Gårding inequality (2.29), with $\mathcal{K} = \mathcal{K}_1 + \mathcal{K}_2$. We obtain from it that $I - \mathcal{L}(V\cdot)$ is the sum of the coercive operator $I - \mathcal{L}(V\cdot) - \mathcal{K}$ and the compact operator \mathcal{K} . Thus, $I - \mathcal{L}(V\cdot)$ is a Fredholm operator [16]. \square

We conclude the discussion on the solvability of the forward problem with the remark that when ε_r is C^1 , one can extend the results in [15] to prove uniqueness of solution of equation (2.28). The existence of the solution follows from the Fredholm property.

3. Data model. Since the array is far away from the support D of the scattering potential V , at coordinate $x_3 = -L$, the results in the previous section give

$$\vec{E}^{sc}(\vec{x}) \approx k^2 \int \mathbb{G}^P(\vec{x}, \vec{y}) \vec{u}(\vec{y}) d\vec{y}, \quad \vec{x} = (x, -L). \quad (3.1)$$

Here

$$\vec{u}(\vec{y}) = V(\vec{y}) \vec{E}(\vec{y}), \quad (3.2)$$

is an effective source supported in D , representing the wave emitted by the unknown reflectors illuminated by the field $\vec{E}(\vec{y})$. The approximation in (3.1) is because we replaced the Green tensor \mathbb{G} defined in Lemma 2.2 by its approximation \mathbb{G}^P which neglects the evanescent waves. Explicitly, if we denote by P the set of indexes of the propagating modes

$$P = \{n \in \mathbb{N}_o^2 : \lambda_n < k^2\},$$

we have

$$\mathbb{G}^P(\vec{x}, \vec{y}) = (\vec{G}_1^P, \vec{G}_2^P, \vec{G}_3^P)(\vec{x}, \vec{y}) + \frac{1}{k^2} \vec{\nabla} \vec{\nabla} \cdot (\vec{G}_1^P, \vec{G}_2^P, \vec{G}_3^P)(\vec{x}, \vec{y}), \quad (3.3)$$

with

$$\vec{G}_j^P(\vec{x}, \vec{y}) = \sum_{n \in P} \sum_{s=1}^{m_n} \frac{\vec{e}_j \cdot \vec{\Phi}_n^{(s)}(\vec{y})}{\|\vec{\Phi}_n^{(s)}\|^2} [e^{i\beta_n(y_3+L)} + (2\delta_{s3} - 1)e^{i\beta_n(L-y_3)}] \frac{\vec{\Phi}_n^{(s)}(\vec{x})}{2i\beta_n}, \quad (3.4)$$

where we used that $x_3 = -L$ at the array.

Let us denote by \mathcal{S}_q the linear mapping from the effective source (3.2) to the q -th component of the scattered field at the array

$$[\mathcal{S}_q(\vec{u})](\vec{x}) = k^2 \int \vec{e}_q \cdot \mathbb{G}^P((\vec{x}, -L), \vec{y}) \vec{u}(\vec{y}) d\vec{y}, 1 \leq q \leq 3. \quad (3.5)$$

Since the support of the source (3.2) is included in D , we may seek to reconstruct the domain D by inverting approximately \mathcal{S}_q . The mapping that takes the scattering potential V to the measurements is nonlinear, because the scattered field E^{sc} enters the definition (3.2). Thus, we linearize it, meaning that we make the single scattering (Born) approximation

$$\vec{u}(\vec{y}) \approx V(\vec{y}) \vec{E}^o(\vec{y}). \quad (3.6)$$

We denote by \mathcal{B} the linear mapping from the scattering potential V to the effective source

$$[\mathcal{B}(V)](\vec{y}) = V(\vec{y}) \vec{E}^o(\vec{y}). \quad (3.7)$$

Then, the forward map \mathcal{F}_q from the scattering potential V to the q -th component of the electric field measured at the array is the composition of the mappings in (3.6) and (3.7),

$$\mathcal{F}_q(V) = \mathcal{S}_q \circ \mathcal{B}(V) \quad (3.8)$$

The data are denoted by $d_q(\vec{x})$, for components $q = 1, \dots, Q$, with $Q \leq 3$, and $\vec{x} \in A$, the aperture of the array, which is a subset of the waveguide cross-section Ω .

4. Imaging. Let \mathbf{d} be the data vector, with entries given by $d_q(\vec{x})$ for all \vec{x} in A and $q = 1, \dots, Q$. Let also \mathbf{V} be the reflectivity vector consisting of the unknown components of the scattering potential V , discretized in the imaging window D_I that contains the unknown support D . Then, we can state the imaging problem as finding an approximate solution \mathbf{V} of the linear system of equations

$$\mathbf{d} = \mathbf{F}\mathbf{V}. \quad (4.1)$$

The reflectivity to data matrix \mathbf{F} is defined by the discretization of the forward mapping (3.8).

The system of equations (4.1) is usually underdetermined, so to find a unique approximation we regularize the inversion by minimizing either the ℓ_2 or the ℓ_1 norm of \mathbf{V} . The first regularization is related to the reverse time migration approach, as described in section 4.1. The imaging with ℓ_1 minimization is discussed in section 4.2.

4.1. Reverse time migration. The minimum ℓ_2 norm solution of (4.1) is

$$\mathbf{V} = \mathbf{F}^\dagger \mathbf{d}, \quad (4.2)$$

where \mathbf{F}^\dagger is the pseudo-inverse of \mathbf{F} . If \mathbf{F} is full row rank, $\mathbf{F}^\dagger = \mathbf{F}^*(\mathbf{F}\mathbf{F}^*)^{-1}$, where the superscript denotes the adjoint. Moreover, if the rows of \mathbf{F} are nearly orthogonal,

which requires proper placement of the receiver locations in the array aperture A , at distance of the order of the wavelength, matrix $\mathbf{F}\mathbf{F}^*$ is nearly diagonal, so by replacing \mathbf{F}^\dagger in (4.2) with \mathbf{F}^* we get a similar answer, up to multiplicative factors. This replacement does not affect the support of the reconstruction and we denote the result by

$$\mathbf{V}^{\text{TR}} = \mathbf{F}^* \mathbf{d}, \quad (4.3)$$

with superscript TR for “time reversal”.

To explain where time reversal comes in, let us compute the adjoint of the forward mapping (3.8). Before discretizing the imaging window we have

$$\begin{aligned} (\mathcal{F}(V), \mathbf{d}) &= \sum_{q=1}^Q \sum_{\mathbf{x} \in A} [\mathcal{F}_q(V)](\mathbf{x}) \overline{d_q(\mathbf{x})} \\ &= k^2 \sum_{q=1}^Q \sum_{\mathbf{x} \in A} \int d\vec{\mathbf{y}} \vec{\mathbf{e}}_q \cdot \mathbb{G}^P((\mathbf{x}, -L), \vec{\mathbf{y}}) V(\vec{\mathbf{y}}) \vec{\mathbf{E}}^o(\vec{\mathbf{y}}) \overline{d_q(\mathbf{x})}, \end{aligned}$$

by the definition (3.8) of the forward map and equation (3.5). We rewrite this as

$$(\mathcal{F}(V), \mathbf{d}) = \sum_{l=1}^3 \int d\vec{\mathbf{y}} [V(\vec{\mathbf{y}}) \vec{\mathbf{E}}^o(\vec{\mathbf{y}})]_l \left[k^2 \sum_{q=1}^Q \sum_{\mathbf{x} \in A} \mathbb{G}_{lq}^P(\vec{\mathbf{y}}, (\mathbf{x}, -L)) \overline{d_q(\mathbf{x})} \right], \quad (4.4)$$

using the Rayleigh-Carson reciprocity relation $\mathbb{G}^P(\vec{\mathbf{x}}, \vec{\mathbf{y}}) = [\mathbb{G}^P(\vec{\mathbf{y}}, \vec{\mathbf{x}})]^T$ of the Green’s tensor. The last factor, in the square brackets, is the electric field evaluated at points $\vec{\mathbf{y}}$ in the imaging window D_I , due to a source at the array which emits the data recordings d_q reversed in time. The time reversal is equivalent to complex conjugation in the Fourier domain. The adjoint of the forward map follows from (4.4),

$$(\mathcal{F}(V), \mathbf{d}) = \sum_{l,m=1}^3 \int V_{lm}(\vec{\mathbf{y}}) E_m^o(\vec{\mathbf{y}}) \left[k^2 \sum_{q=1}^Q \sum_{\mathbf{x} \in A} \mathbb{G}_{lq}^P(\vec{\mathbf{y}}, (\mathbf{x}, -L)) \overline{d_q(\mathbf{x})} \right] = (V, \mathcal{F}^*(\mathbf{d})),$$

where the inner product in the right hand side is

$$(V, U) = \int d\vec{\mathbf{y}} \text{trace}[V(\vec{\mathbf{y}})U(\vec{\mathbf{y}})],$$

for any complex valued matrix U . Recall that $V(\vec{\mathbf{y}})$ is Hermitian. Thus, $\mathcal{F}^*(\mathbf{d})$ is a 3×3 complex matrix valued field, with components

$$[\mathcal{F}^*(\mathbf{d})]_{ml}(\vec{\mathbf{y}}) = \left[k^2 \sum_{q=1}^Q \sum_{\mathbf{x} \in A} \mathbb{G}_{lq}^P(\vec{\mathbf{y}}, (\mathbf{x}, -L)) \overline{d_q(\mathbf{x})} \right] E_m^o(\vec{\mathbf{y}}). \quad (4.5)$$

The right hand side in the imaging formula (4.3) is the discretization of (4.5) over points $\vec{\mathbf{y}}$ in the imaging window.

In the particular case of a diagonal scattering potential $V(\vec{\mathbf{y}})$, which corresponds to the coordinate axes being the same as the principal axes of the dielectric material in the support of the reflectors, the adjoint operator acts from the data space to the space of diagonal, positive definite matrices. The reconstruction is given by

$$V_{ll}^{\text{TR}}(\vec{\mathbf{y}}) = \left[k^2 \sum_{q=1}^Q \sum_{\mathbf{x} \in A} \mathbb{G}_{lq}^P(\vec{\mathbf{y}}, (\mathbf{x}, -L)) \overline{d_q(\mathbf{x})} \right] E_l^o(\vec{\mathbf{y}}), \quad (4.6)$$

where \vec{y} are the discretization points in D_I . Moreover, if the material is isotropic, so that V is a multiple of the identity, the reconstruction is $V^{\text{TR}} I$, with

$$V^{\text{TR}}(\vec{y}) = \sum_{l=1}^3 \left[k^2 \sum_{q=1}^Q \sum_{\mathbf{x} \in A} \mathbb{G}_{lq}^P(\vec{y}, (\mathbf{x}, -L)) \overline{d_q(\mathbf{x})} \right] E_l^o(\vec{y}). \quad (4.7)$$

None of these formulae are quantitative approximations of V , so we may drop the factor k^2 and display their absolute values at points \vec{y} in the imaging window D_I . The estimate of the support D of V is given by the subset in D_I where the displayed values are large.

4.2. Imaging with ℓ_1 optimization. To incorporate the prior information that the reflectors have small support in the imaging window, we may reconstruct the scattering potential using ℓ_1 optimization. This means solving the optimization problem

$$\min \|\mathbf{V}\|_{\ell_1} \quad \text{such that} \quad \mathbf{d} = \mathbf{F}\mathbf{V}. \quad (4.8)$$

The equality constraint may be replaced by the inequality $\|\mathbf{d} - \mathbf{F}\mathbf{V}\|_{\ell_2}^2 \leq$ some user defined tolerance, which deals better with measurement and modeling noise. The ℓ_1 optimization is carried with the cvx package “<http://cvxr.com/cvx/>”.

5. Numerical simulations. We present in this section examples of reconstructions of the reflectors with reverse time migration and ℓ_1 optimization. The simulations are for a waveguide with cross-section $\Omega = (0, 13.9\lambda) \times (0, 14.2\lambda)$, and the array is at distance $L = 41.8\lambda$ from the end wall, where λ is the wavelength. The source density in (1.1) is

$$\vec{\mathbf{J}}(\mathbf{x}) = \vec{p} \delta(\mathbf{x} - (6.95, 7.1)\lambda), \quad (5.1)$$

for constant vector \vec{p} , and the receiver sensors are located at uniform spacing of approximately $\lambda/18$ in the array aperture A . We present results with full aperture, where $A = \Omega$ and with 75% aperture, where $A \subset \Omega$ is a rectangle of sides 10.5λ and 10.65λ , with center at the waveguide axis. The receivers measure only the 2–nd component of $\vec{\mathbf{E}}^{sc}$. We compared the results with those obtained from all components of $\vec{\mathbf{E}}^{sc}$ at the array, and the images were essentially the same.

The images displayed in Figures 5.1–5.4 are obtained with an approximation of the formulae in section 4, where only a subset of the 648 propagating modes are used. This is because in practice the sensors record over a finite time window, and only the modes that propagate fast enough to arrive at the array during the duration of the measurements contribute. The polarization vector \vec{p} in (5.1) equals $(0, 1, 0)^T$ in the simulations with isotropic permittivity and $(1, 1, 1)^T$ in the case of anisotropic permittivity.

In figure 5.1 we display the reverse time migration image of a point-like reflector located at $(6.95, 4.73, -10.44)\lambda$, modeled by an isotropic scattering potential $V = v(\vec{y})I$ supported on a mesh cell in the imaging region. The mesh size is $\lambda/18$ in cross-range plane and $\lambda/6$ in range. We note that the reflector is well localized in range and cross-range, and the results improve, as expected when more modes are used to form the image. Moreover, the image at 75% aperture is almost as good as that with full aperture. Naturally, the image deteriorates for smaller apertures.

The images of the same reflector obtained with ℓ_1 optimization are shown in Figure 5.2. They are obtained with the first 350 arriving modes and a 75% aperture.

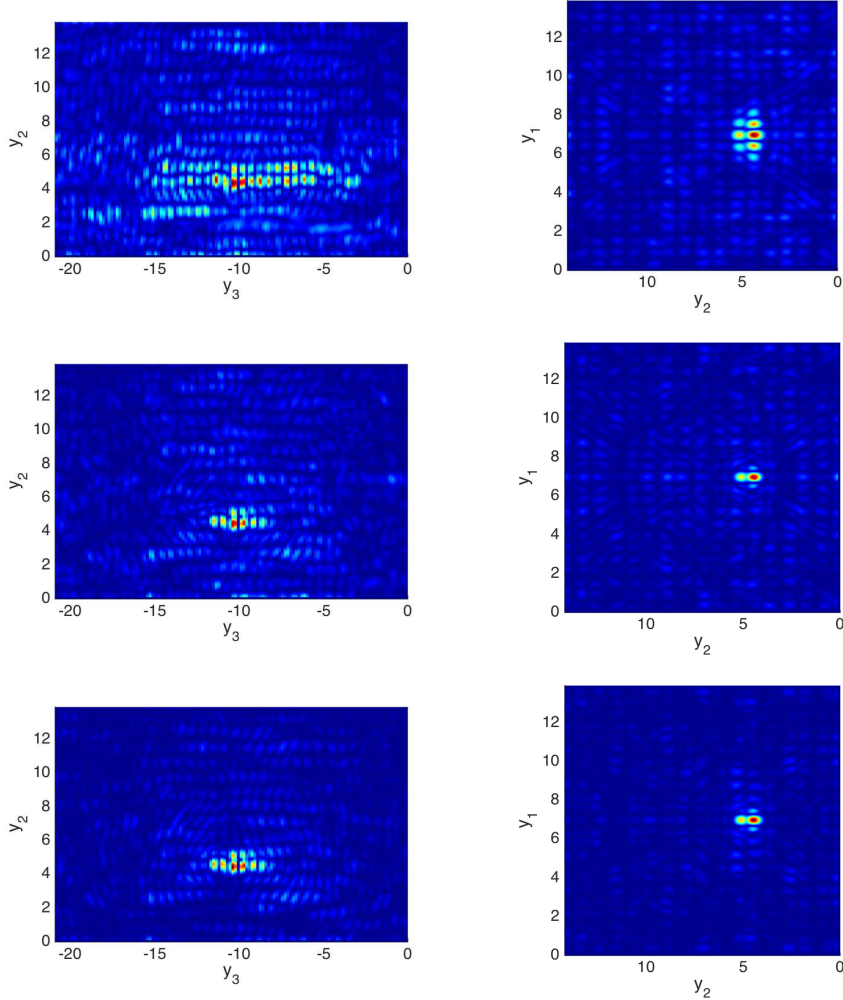


Figure 5.1: Reverse time migration images of a point-like reflector located at $(6.95, 4.73, -10.44)\lambda$. The images in the first two rows are with 75% aperture and those in the last row with the full aperture. The first row is for 100 modes and the other two rows for 350 modes. We display in the left column the images in the plane $y_1 = 6.95\lambda$, and in the right column the images in the cross-range plane $y_3 = -10.44\lambda$. The axes are in units of λ .

The discretization of these images is in steps of 0.29λ in cross-range and 0.87λ in range. As expected, these images give a sharper estimate of the support, in the sense that the spurious faint peaks in Figure 5.1 are suppressed in Figure 5.2 by the sparsity promoting optimization.

In Figures 5.3 and 5.4 we show images of an extended reflector shaped like a rectangular shell of sides equal to $1.16\lambda, 1.18\lambda$ and 3.9λ . The shell is modeled as $R \setminus R_o$, where $R = (6.38\lambda, 7.54\lambda) \times (6.51\lambda, 7.69\lambda) \times (-13.09\lambda, -9.19\lambda)$ and $R_o = (6.09\lambda, 7.25\lambda) \times (6.22\lambda, 7.40\lambda) \times (-12.22\lambda, -8.32\lambda)$. The scattering potential equals

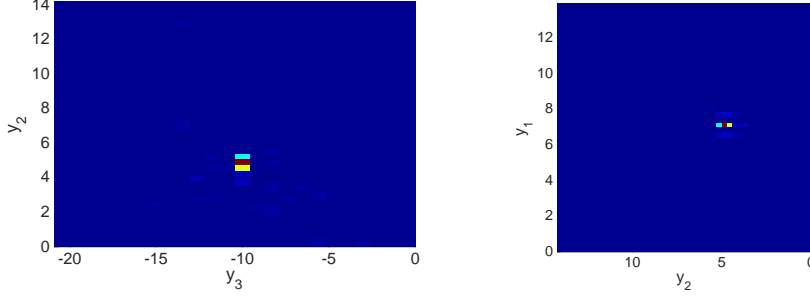


Figure 5.2: Reconstructions of the same reflector as in Figure 5.1 using ℓ_1 optimization, 350 modes and 75% aperture. The axes are in units of λ .

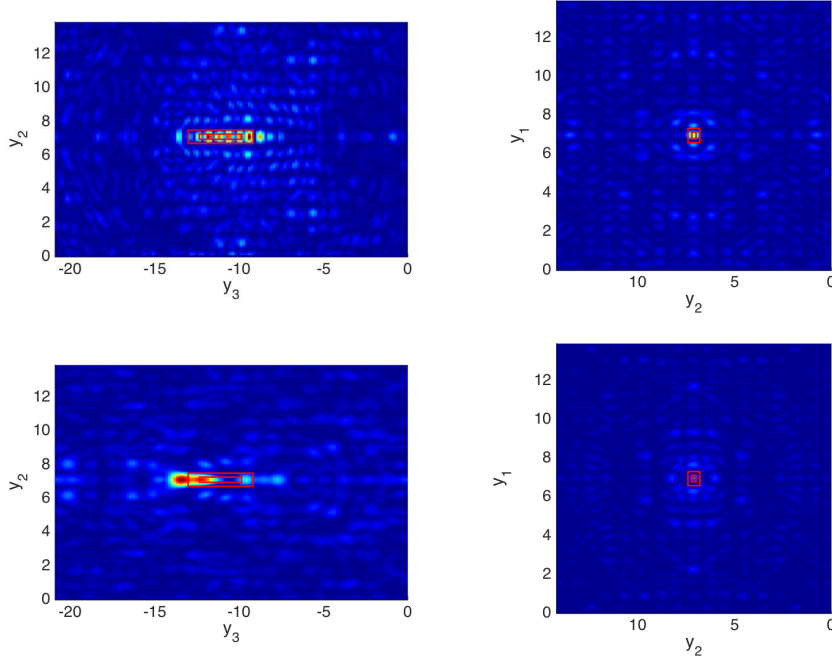


Figure 5.3: Reverse time migration images of a rectangular shell. The results in the first row are in the terminated waveguide. Those in the second row are in an infinite waveguide. We use the 350 first arriving modes, 75% aperture. The images in the left column are in the plane $y_1 = 6.96\lambda$ and in the right column in the cross-range plane at $y_3 = -11.14\lambda$.

8 in $R \setminus R_o$ and zero outside, while the thickness of the cross-range and range walls are 0.87λ and 0.29λ , respectively. The discretization of the imaging window in Figure 5.3 is the same as in Figure 5.1. We note that the reverse time migration method estimates better the support of the reflector, specially its back, in the terminating waveguide (top left image) than in the infinite waveguide (bottom left image). The ℓ_1 optimization images are in Figure 5.4, where the discretization of the imaging window

is the same as in Figure 5.2.

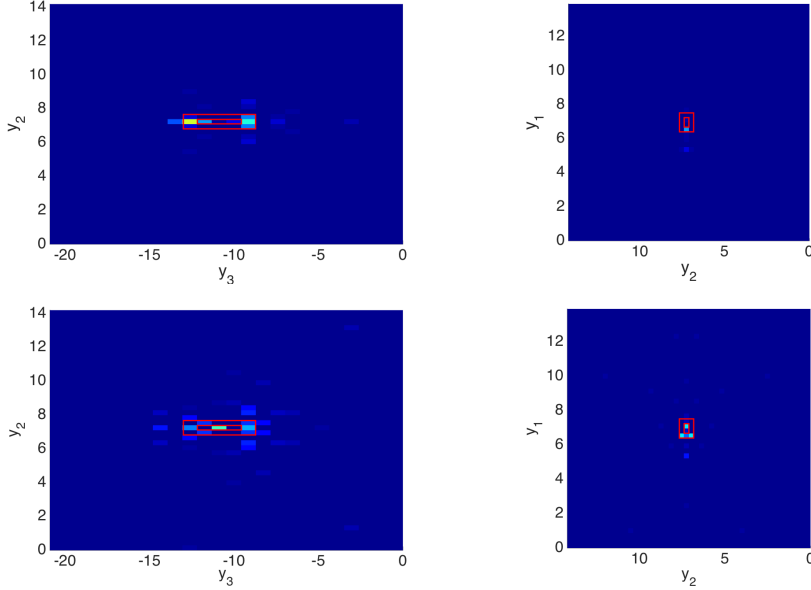


Figure 5.4: Reconstructions of the same rectangle shell as in Figure 5.3, using ℓ_1 optimization, 350 modes and 75% aperture. In the top line we show the images in the terminating waveguide and in the bottom line those in the infinite waveguide. The images in the left column are in the plane $y_1 = 6.96\lambda$ and in the right column in the cross-range plane at $y_3 = -11.14\lambda$.

In the last simulations in Figure 5.5 we present the images of an anisotropic point-like reflector, whose scattering potential is a diagonal matrix $V(\vec{y}) = \text{diag}(3, 1, 5)v(\vec{y})$, with the same $v(\vec{y})$ as in Figure 5.1. We present only reverse time migration images and note that the estimates of the support of the components of $V(\vec{y})$ are similar to those in Figure 5.1. Specifically, we plot the absolute value of the right hand side of equation (4.6) for $l = 1, 2, 3$.

6. Summary. We study imaging with electromagnetic waves in terminating waveguides, using measurements of the electric field at an array of sensors. The goal of imaging is to localize compactly supported reflectors that lie between the array and the end wall. We derive the data model using Maxwell's equations. We define the scattered electric field due to an incident wave from one sensor in the array and show that it satisfies a Lipmann-Schwinger type equation. We analyze the solvability of this equation and write explicitly the data model using a modal decomposition of the wave field in the waveguide. This model is based on the single scattering approximation at the unknown reflectors. We use it to formulate two imaging methods: The first forms an image by calculating the action of the adjoint of the forward operator on the data. It has a time reversal interpretation. The second uses ℓ_1 i.e., sparsity enhancing optimization. We present numerical results with both imaging methods for point-like and extended reflectors.

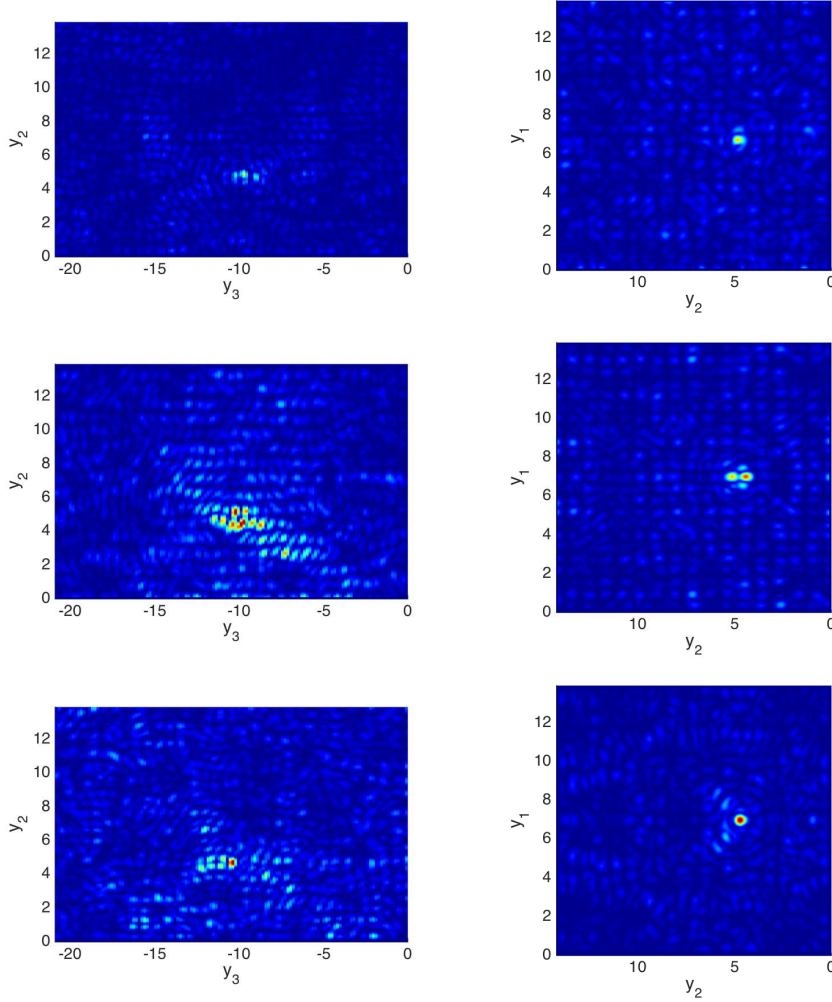


Figure 5.5: Reverse time migration images of an anisotropic point-like reflector located at $(6.95, 4.73, -10.44)\lambda$, using reverse time migration. We use the first 350 arriving modes and 75% aperture. We display the absolute value of (4.6) for $l = 1$ in the first line, 2 in the second and 3 in the third. The images in the left column are in the plane $y_1 = 6.95\lambda$ and in the right column in the plane $y_3 = -10.44\lambda$. The axes are in units of λ .

Acknowledgements. This work was partially supported by AFOSR Grant FA9550-12-1-0117 (DLN) and AFOSR grant FA9550-15-1-0118 (LB). LB also acknowledges support from the Simons Foundation and ONR Grant N000141410077.

Appendix A. Vectorial eigenvalue problem.

A.1. Spectral decomposition of the Laplacian. Let $\vec{f} = (f, f_3)^\top \in (L^2(\Omega))^3$, and consider the linear differential operator associated with the vectorial

Laplacian problem

$$\begin{aligned} -\Delta \vec{\mathbf{u}}(\mathbf{x}) &= \vec{\mathbf{f}}(\mathbf{x}) \quad \mathbf{x} \in \Omega, \\ \mathbf{n}^\perp(\mathbf{x}) \cdot \mathbf{u}(\mathbf{x}) &= \nabla \cdot \mathbf{u}(\mathbf{x}) = 0 \quad \mathbf{x} \in \partial\Omega, \end{aligned} \quad (\text{A.1})$$

$$u_3(\mathbf{x}) = 0 \quad \mathbf{x} \in \partial\Omega, \quad (\text{A.2})$$

for $\vec{\mathbf{u}} = (\mathbf{u}, u_3)$. Since $\Delta \vec{\mathbf{u}} = (\Delta \mathbf{u}, \Delta u_3)^\top$, we have two decoupled problems. One is the standard Poisson problem for the longitudinal component u_3 ,

$$\begin{aligned} -\Delta u_3(\mathbf{x}) &= f_3(\mathbf{x}) \quad \mathbf{x} \in \Omega, \\ u_3(\mathbf{x}) &= 0 \quad \mathbf{x} \in \partial\Omega, \end{aligned} \quad (\text{A.3})$$

whose weak solution is in $H_0^1(\Omega)$ and satisfies

$$b(u_3, v) = \int_{\Omega} \nabla u_3(\mathbf{x}) \cdot \nabla \bar{v}(\mathbf{x}) \, d\mathbf{x} = (f_3, v)_{L^2}, \quad \text{for all } v \in \mathbf{H}_0^1(\Omega), \quad (\text{A.4})$$

where $(\cdot, \cdot)_{L^2}$ denotes the inner product in $L^2(\Omega)$. The other problem is for the two dimensional transverse vector \mathbf{u} ,

$$\begin{aligned} -\Delta \mathbf{u}(\mathbf{x}) &= \mathbf{f}(\mathbf{x}) \quad \mathbf{x} \in \Omega, \\ \mathbf{n}^\perp(\mathbf{x}) \cdot \mathbf{u}(\mathbf{x}) &= 0 \quad \mathbf{x} \in \partial\Omega, \\ \nabla \cdot \mathbf{u}(\mathbf{x}) &= 0 \quad \mathbf{x} \in \partial\Omega. \end{aligned} \quad (\text{A.5})$$

It is studied in [14] for a more general Ω than the rectangle considered here. The results there establish the existence and uniqueness of weak solutions in the space

$$\mathbf{H}_{0t}^1(\Omega) = \{\mathbf{u} \in (H^1(\Omega))^2 : \mathbf{n}^\perp \cdot \mathbf{u} = 0 \text{ on } \partial\Omega\},$$

with the standard inner H^1 product $(\mathbf{u}, \mathbf{v})_{H^1}$. These solutions satisfy the variational problem

$$a(\mathbf{u}, \mathbf{v}) = \int_{\Omega} (\nabla^\perp \cdot \mathbf{u}(\mathbf{x}) \nabla^\perp \cdot \bar{\mathbf{v}}(\mathbf{x}) + \nabla \cdot \mathbf{u}(\mathbf{x}) \nabla \cdot \bar{\mathbf{v}}(\mathbf{x})) \, d\mathbf{x} = (\mathbf{f}, \mathbf{v})_{L^2}, \quad (\text{A.6})$$

for all $\mathbf{v} \in \mathbf{H}_{0t}^1(\Omega)$, where ∇^\perp is the rotated gradient operator, playing the role of curl in two-dimensions, and $(\cdot, \cdot)_{L^2}$ is the inner product in $(L^2(\Omega))^2$. The results in [14] also give a proper interpretation of $\nabla \cdot \mathbf{u}|_{\partial\Omega}$ in terms of the curvature of the boundary. In our case the boundary is the union of four line segments $\partial\Omega_j$, for $j = 1, \dots, 4$, so the curvature is zero on each segment. It is shown in [14] that $\nabla \cdot \mathbf{u}|_{\partial\Omega}$ exists and belongs to $H^{-1/2}(\partial\Omega_j)$ on each piece of the boundary, and the weak solution satisfies the estimate

$$\|\mathbf{u}\|_{H^1} \leq C \|\mathbf{f}\|_{L^2}. \quad (\text{A.7})$$

To arrive at the spectral decomposition of the vectorial Laplacian in (A.2), we study its “inverse” i.e., the solution operator $\mathcal{L} : (L^2(\Omega))^3 \rightarrow (L^2(\Omega))^3$ defined by $\mathcal{L}(\vec{\mathbf{f}}) = (\mathbf{u}, u_3)$, where \mathbf{u} solves (A.6) and u_3 solves (A.4). Obviously, \mathcal{L} is a linear operator. It is also injective, bounded, self-adjoint and compact. The injectivity follows from the uniqueness of solutions of (A.4) and (A.6). The boundedness and compactness follow from the estimate (A.7) on \mathbf{u} and a similar one on u_3 , together

with the imbedding of $H_{0t}^1(\Omega)$ in $(L^2(\Omega))^2$ and of $H_0^1(\Omega)$ in $L^2(\Omega)$. To see that \mathcal{L} is self-adjoint, let \vec{f} and \vec{g} be arbitrary in $(L^2(\Omega))^3$ and denote by (\mathbf{u}, u_3) and (\mathbf{v}, v_3) their image in $\text{Im}(\mathcal{L}) \subset (L^2(\Omega))^3$, such that $\mathcal{L}(\vec{f}) = (\mathbf{u}, u_3)$ and $\mathcal{L}(\vec{g}) = (\mathbf{v}, v_3)$. Then equations (A.4) and (A.6) give

$$\begin{aligned} (\mathcal{L}(\vec{f}), \vec{g})_{L^2} &= (\mathbf{u}, \mathbf{g})_{L^2} + (u_3, g_3)_{L^2} = \overline{a(\mathbf{v}, \mathbf{u})} + \overline{b(v_3, u_3)} \\ &= a(\mathbf{u}, \mathbf{v}) + b(u_3, v_3) = (\mathbf{f}, \mathbf{v})_{L^2} + (f_3, v_3)_{L^2} \\ &= (\vec{f}, \mathcal{L}(\vec{g}))_{L^2}. \end{aligned}$$

We conclude from the spectral theorem for self-adjoint, compact operators [10, appendix D] that there is an orthogonal basis of $(L^2(\Omega))^3$ consisting of the eigenfunctions \vec{u}_j of \mathcal{L} , for eigenvalues γ_j that tend to 0 as $j \rightarrow \infty$.

The eigenvalues cannot be zero, because \mathcal{L} is injective, so we can divide by them and get

$$\vec{u}_j = \gamma_j^{-1} \mathcal{L}(\vec{u}_j).$$

Consequently, by estimate (A.7) and a similar one for the standard problem (A.4), we obtain that $\vec{u}_j = (\mathbf{u}_j, u_{3,j}) \in \mathcal{H}$, the space of three dimensional vectors with components $\mathbf{u}_j \in H_{0t}^1(\Omega)$ and $u_{3,j} \in H_0^1(\Omega)$. To finish the argument, let $\vec{v} = (\mathbf{v}, v_3) \in \mathcal{H}$ and consider the bilinear form $A : \mathcal{H} \times \mathcal{H} \rightarrow \mathbb{C}$ defined in the obvious way

$$A(\vec{u}, \vec{v}) = a(\mathbf{u}, \mathbf{v}) + b(u_3, v_3).$$

By letting $\vec{u} = \vec{u}_j$ we get

$$\gamma_j A(\vec{u}_j, \vec{v}) = A(\mathcal{L}(\vec{u}_j), \vec{v}) = (\mathbf{u}_j, \mathbf{v})_{L^2} + (u_{3,j}, v_3)_{L^2} = \langle \vec{u}_j, \vec{v} \rangle,$$

where we used equations (A.4) and (A.6) and recall that $\langle \cdot, \cdot \rangle$ is the inner product in $(L^2(\Omega))^3$. This relation states that \vec{u}_j are weak eigenfunctions of the vectorial Laplacian, for eigenvalues $\lambda_j = \gamma_j^{-1}$.

Finally, the expression (2.6) of the eigenvalues and (2.8)–(2.11) of the eigenfunctions follow by direct calculation i.e., the method of separation of variables. See [1, section 3]. The eigenfunctions \vec{u}_j are denoted in the paper by $\vec{\Phi}_j^{(s)}(\mathbf{x})$, with index $s = 1, \dots, m_j$, the multiplicity of the eigenvalue λ_j .

Appendix B. The reference field. Because the eigenfunctions $\vec{\Phi}_j^{(s)}(\mathbf{x})$ are an orthogonal basis, we can seek the solution \vec{E}^o of equations (2.1) in the form

$$\vec{E}^o(\vec{x}) = \sum_{j \in \mathbb{N}_0^2} \sum_{s=1}^{m_j} g_j^{(s)}(x_3) \vec{\Phi}_j^{(s)}(\mathbf{x}), \quad (\text{B.1})$$

for each given $x_3 < 0$. It remains to determine the coefficients $g_j^{(s)}(x_3)$.

We substitute (B.1) in (2.1), and calculating

$$\begin{aligned} \vec{\nabla} \times \vec{\nabla} \times \left[g_n^{(1)}(x_3) \vec{\Phi}_j^{(1)}(\mathbf{x}) \right] &= [\lambda_n g_n^{(1)}(x_3) - \partial_{x_3} g_j^{(1)}(x_3)] \vec{\Phi}_j^{(1)}(\mathbf{x}), \\ \vec{\nabla} \times \vec{\nabla} \times \left[g_n^{(2)}(x_3) \vec{\Phi}_j^{(2)}(\mathbf{x}) \right] &= -\partial_{x_3}^2 g_j^{(2)}(x_3) \vec{\Phi}_j^{(2)}(\mathbf{x}) - \lambda_j \partial_{x_3} g_j^{(2)}(x_3) \vec{\Phi}_j^{(3)}(\mathbf{x}), \\ \vec{\nabla} \times \vec{\nabla} \times \left[g_n^{(3)}(x_3) \vec{\Phi}_j^{(3)}(\mathbf{x}) \right] &= \lambda_j g_j^{(3)}(x_3) \vec{\Phi}_j^{(3)}(\mathbf{x}) + \partial_{x_3} g_j^{(3)}(x_3) \vec{\Phi}_j^{(2)}(\mathbf{x}), \end{aligned} \quad (\text{B.2})$$

we get

$$\begin{aligned}
i\omega\mu_o\vec{\mathbf{J}}(\mathbf{x})\delta(x_3+L) = \sum_{j \in \mathbb{N}_0^2} \sum_{s=1}^{m_j} \Big\{ & [(\lambda_j - k^2)g_j^{(1)}(x_3) - \partial_{x_3}^2 g_j^{(1)}(x_3)] \vec{\Phi}_j^{(1)}(\mathbf{x})\delta_{s,1} \\
& + [-(k^2 + \partial_{x_3}^2)g_j^{(2)}(x_3) + \partial_{x_3} g_j^{(3)}(x_3)] \vec{\Phi}_j^{(2)}(\mathbf{x})\delta_{s,2} \\
& + [(\lambda_j - k^2)g_j^{(3)}(x_3) - \lambda_j \partial_{x_3} g_j^{(2)}(x_3)] \vec{\Phi}_j^{(3)}(\mathbf{x})\delta_{s,3} \Big\}. \quad (\text{B.3})
\end{aligned}$$

The equations for $g_j^{(s)}(x_3)$ follow from (B.3) and the orthogonality of the eigenfunctions,

$$\begin{aligned}
\partial_{x_3}^2 g_j^{(1)}(x_3) &= -(k^2 - \lambda_j)g_j^{(1)}(x_3), \\
\partial_{x_3}^2 g_j^{(2)}(x_3) &= -(k^2 - \lambda_j)g_j^{(2)}(x_3), \\
g_j^{(3)}(x_3) &= \frac{\lambda_j}{\lambda_j - k^2} \partial_{x_3} g_j^{(2)}(x_3), \quad x_3 \neq -L.
\end{aligned}$$

The solution of these equations is

$$g_j^{(s)}(x_3) = a_j^{\pm(s)} e^{i\beta_j x_3} + b_j^{\pm(s)} e^{-i\beta_j x_3}, \quad \text{for } s = 1, 2, \quad (\text{B.4})$$

and

$$g_j^{(3)}(x_3) = \frac{\lambda_j}{\lambda_j - k^2} \left[i\beta_j a_j^{\pm(s)} e^{i\beta_j x_3} - i\beta_j b_j^{\pm(s)} e^{-i\beta_j x_3} \right], \quad (\text{B.5})$$

where \pm stands for the right and left of source. The amplitudes $a_j^{\pm(s)}$ and $b_j^{\pm(s)}$ have the expression given in (2.14)-(2.17). They are derived from the jump conditions at the source,

$$\begin{aligned}
-\left[\partial_{x_3} g_j^{(1)}\right]_{-L} &= \frac{i\omega\mu_o(\vec{\Phi}_j^{(1)}, \vec{\mathbf{J}})}{\|\vec{\Phi}_j^{(1)}\|^2}, \quad \left[g_j^{(1)}\right]_{-L} = 0, \\
-\left[\partial_{x_3} g_j^{(2)}\right]_{-L} + \left[g_j^{(3)}\right]_{-L} &= \frac{i\omega\mu_o(\vec{\Phi}_j^{(2)}, \vec{\mathbf{J}})}{\|\vec{\Phi}_j^{(2)}\|^2}, \\
-\lambda_j \left[g_j^{(2)}\right]_{-L} &= \frac{i\omega\mu_o(\vec{\Phi}_j^{(3)}, \vec{\mathbf{J}})}{\|\vec{\Phi}_j^{(3)}\|^2},
\end{aligned}$$

the boundary conditions $\vec{\mathbf{e}}_3 \times \vec{\mathbf{E}}^o|_{x_3=0} = 0$, which imply

$$\begin{aligned}
a_j^{+(1)} + b_j^{+(1)} &= 0, \\
a_j^{+(2)} + b_j^{+(2)} &= 0,
\end{aligned}$$

and the radiation conditions $a_j^{-(1)} = a_j^{-(2)} = 0$ for $x_3 < -L$.

Appendix C. Derivation of the dyadic Green's function. It is straightforward to check that \mathbb{G} given in (2.23) satisfies equation (2.22), provided that \vec{G}_j

satisfies (2.25). To calculate \vec{G}_j , we make the following observations. On $\partial\Omega$, where $\vec{n} = (\mathbf{n}, 0)$,

$$\vec{n} \times \vec{\Phi}_j^{(s)} = -[(\mathbf{n}^\perp, 0) \cdot \vec{\Phi}_j^{(s)}] \vec{e}_3 = 0, \text{ for } s = 1, 2, \text{ and } \vec{n} \times \vec{\Phi}_j^{(3)} = 0.$$

Moreover, for a regular function $g(x_3)$ we have

$$\begin{aligned} \vec{\nabla}[\vec{\nabla} \cdot (g(x_3) \vec{\Phi}_j^{(1)}(\mathbf{x}))] &= 0, \\ \vec{\nabla}[\vec{\nabla} \cdot (g(x_3) \vec{\Phi}_j^{(2)}(\mathbf{x}))] &= -\lambda_j g(x_3) \vec{\Phi}_j^{(2)}(\mathbf{x}) - \lambda_j \partial_{x_3} g(x_3) \vec{\Phi}_j^{(3)}(\mathbf{x}), \\ \vec{\nabla}[\vec{\nabla} \cdot (g(x_3) \vec{\Phi}_j^{(3)}(\mathbf{x}))] &= \partial_{x_3} g(x_3) \vec{\Phi}_j^{(2)}(\mathbf{x}) + \partial_{x_3}^2 g(x_3) \vec{\Phi}_j^{(3)}(\mathbf{x}). \end{aligned}$$

These observations imply that for all s and $\vec{x} = (\mathbf{x}, x_3)$, with $\mathbf{x} \in \partial\Omega$,

$$\vec{n}(\vec{x}) \times \vec{\nabla}[\vec{\nabla} \cdot (g(x_3) \vec{\Phi}_j^{(s)}(\mathbf{x}))] = \vec{n}(\vec{x}) \times [g(x_3) \vec{\Phi}_j^{(s)}(\mathbf{x})] = 0.$$

This allows us to seek $\vec{G}_j(\cdot, \vec{y})$ as an expansion in the orthogonal basis $\{\vec{\Phi}_n^{(s)}(\mathbf{x})\}$ of eigenfunctions of the vectorial Laplacian

$$\vec{G}_j(\vec{x}, \vec{y}) = \sum_{n \in \mathbb{N}_0^2} \sum_{s=1}^{m_n} g_n^{j(s)}(x_3, \vec{y}) \vec{\Phi}_n^{(s)}(\mathbf{x}), \quad (\text{C.1})$$

because each term satisfies the required boundary conditions at $\partial\Omega$.

Substituting (C.1) in (2.25) gives

$$\sum_{n \in \mathbb{N}_0^2} \sum_{s=1}^{m_n} [\partial_{x_3}^2 g_n^{j(s)}(x_3, \vec{y}) + (k^2 - \lambda_n) g_n^{j(s)}(x_3, \vec{y})] \vec{\Phi}_n^{(s)}(\mathbf{x}) = \delta(\mathbf{x} - \mathbf{y}) \vec{e}_j \delta(x_3 - y_3),$$

and using the orthogonality of the eigenfunctions we obtain the following ordinary differential equations

$$\partial_{x_3}^2 g_n^{j(s)}(x_3, \vec{y}) + (k^2 - \lambda_n) g_n^{j(s)}(x_3, \vec{y}) = \frac{\vec{e}_j \cdot \vec{\Phi}_n^{(s)}(\mathbf{y})}{\|\vec{\Phi}_n^{(s)}\|^2} \delta(x_3 - y_3).$$

The solutions of these equations, which satisfy the radiation condition at $x_3 < y_3$, are

$$g_n^j(x_3, \vec{y}) = \begin{cases} (a_n^{(s)} e^{i\beta_n x_3} + b_n^{(s)} e^{-i\beta_n x_3}) \vec{e}_j \cdot \vec{\Phi}_n^{(s)}(\mathbf{y}) / \|\vec{\Phi}_n^{(s)}\|^2, & x_3 > y_3, \\ c_n^{(s)} e^{-i\beta_n x_3} \vec{e}_j \cdot \vec{\Phi}_n^{(s)}(\mathbf{y}) / \|\vec{\Phi}_n^{(s)}\|^2, & x_3 < y_3. \end{cases} \quad (\text{C.2})$$

The coefficients $a_n^{(s)}$, $b_n^{(s)}$ and $c_n^{(s)}$ are determined by jump conditions at y_3

$$\begin{aligned} g_n^{j(s)}(y_3^+, \vec{y}) - g_n^{j(s)}(y_3^-, \vec{y}) &= 0, \\ \partial_{x_3} g_n^{j(s)}(y_3^+, \vec{y}) - \partial_{x_3} g_n^{j(s)}(y_3^-, \vec{y}) &= \frac{\vec{e}_j \cdot \vec{\Phi}_n^{(s)}(\mathbf{y})}{\|\vec{\Phi}_n^{(s)}\|^2}, \end{aligned} \quad (\text{C.3})$$

and at $x_3 = 0$,

$$\vec{e}_3 \times (k^2 + \vec{\nabla} \vec{\nabla} \cdot) \vec{G}_j(\vec{x}, \vec{y}) = 0. \quad (\text{C.4})$$

The jump conditions (C.3) imply

$$\begin{aligned} a_n^{(s)} e^{i\beta_n y_3} + b_n^{(s)} e^{-i\beta_n y_3} - c_n^{(s)} e^{-i\beta_n y_3} &= 0, \\ a_n^{(s)} e^{i\beta_n y_3} - b_n^{(s)} e^{-i\beta_n y_3} + c_n^{(s)} e^{-i\beta_n y_3} &= \frac{1}{i\beta_n}. \end{aligned} \quad (\text{C.5})$$

For the boundary condition (C.4), we need the formulae

$$\begin{aligned} \vec{e}_3 \times \vec{\Phi}_n^{(1)} &= \begin{pmatrix} \frac{\pi n_1}{L_1} \sin\left(\frac{\pi n_1 x_1}{L_1}\right) \cos\left(\frac{\pi n_2 x_2}{L_2}\right) \\ \frac{\pi n_2}{L_2} \cos\left(\frac{\pi n_1 x_1}{L_1}\right) \sin\left(\frac{\pi n_2 x_2}{L_2}\right) \\ 0 \end{pmatrix}, \\ \vec{e}_3 \times \vec{\Phi}_n^{(2)} &= \begin{pmatrix} -\frac{\pi n_2}{L_2} \sin\left(\frac{\pi n_1 x_1}{L_1}\right) \cos\left(\frac{\pi n_2 x_2}{L_2}\right) \\ \frac{\pi n_1}{L_1} \cos\left(\frac{\pi n_1 x_1}{L_1}\right) \sin\left(\frac{\pi n_2 x_2}{L_2}\right) \\ 0 \end{pmatrix}, \\ \vec{e}_3 \times \vec{\Phi}_n^{(3)} &= 0, \end{aligned}$$

and

$$\begin{aligned} \vec{e}_3 \times \vec{\nabla} [\vec{\nabla} \cdot (g_n^{j(1)}(x_3) \vec{\Phi}_n^{(1)}(\mathbf{x}))] &= 0, \\ \vec{e}_3 \times \vec{\nabla} [\vec{\nabla} \cdot (g_n^{j(2)}(x_3) \vec{\Phi}_n^{(2)}(\mathbf{x}))] &= -\lambda_n g_n^{j(2)}(x_3) \begin{pmatrix} -\frac{\pi n_2}{L_2} \sin\left(\frac{\pi n_1 x_1}{L_1}\right) \cos\left(\frac{\pi n_2 x_2}{L_2}\right) \\ \frac{\pi n_1}{L_1} \cos\left(\frac{\pi n_1 x_1}{L_1}\right) \sin\left(\frac{\pi n_2 x_2}{L_2}\right) \\ 0 \end{pmatrix}, \\ \vec{e}_3 \times \vec{\nabla} [\vec{\nabla} \cdot (g_n^{j(3)}(x_3) \vec{\Phi}_j^{(3)}(\mathbf{x}))] &= \partial_{x_3} g_n^{j(3)}(x_3) \begin{pmatrix} -\frac{\pi n_2}{L_2} \sin\left(\frac{\pi n_1 x_1}{L_1}\right) \cos\left(\frac{\pi n_2 x_2}{L_2}\right) \\ \frac{\pi n_1}{L_1} \cos\left(\frac{\pi n_1 x_1}{L_1}\right) \sin\left(\frac{\pi n_2 x_2}{L_2}\right) \\ 0 \end{pmatrix}. \end{aligned}$$

Substituting in (C.4) we get

$$g_n^{j(1)}(0, \vec{y}) = 0 \text{ and } (k^2 - \lambda_n) g_n^{j(2)}(0, \vec{y}) + \partial_{x_3} g_n^{j(3)}(0, \vec{y}) = 0,$$

or, equivalently,

$$a_n^{(1)} + b_n^{(1)} = 0, \quad (\text{C.6})$$

and

$$(k^2 - \lambda_n)(a_n^{(2)} + b_n^{(2)}) \frac{\vec{e}_j \cdot \vec{\Phi}_j^{(2)}(\vec{y})}{\|\vec{\Phi}_j^{(2)}\|^2} + i\beta_n(a_n^{(3)} - b_n^{(3)}) \frac{\vec{e}_j \cdot \vec{\Phi}_j^{(3)}(\vec{y})}{\|\vec{\Phi}_j^{(3)}\|^2} = 0. \quad (\text{C.7})$$

We now have a linear system of eight equations (C.5), (C.6) and (C.7) for the nine unknowns $a_n^{(s)}$, $b_n^{(s)}$ and $c_n^{(s)}$. The system is underdetermined, so \vec{G}_j is not uniquely defined. However, $\mathbb{G}(\cdot, \vec{y})$ given by (2.23) is unique, because a straightforward computation shows that the coefficients with $s = 2$ or 3 appear only in the combinations

$$(b_n^{(3)} + i\beta_n b_n^{(2)}) \left(\vec{\Phi}_n^{(2)} + \frac{i\lambda_n}{\beta_n} \vec{\Phi}_n^{(3)}(\mathbf{x}) \right) e^{-i\beta_n x_3}$$

and

$$(a_n^{(3)} - i\beta_n a_n^{(2)}) \left(\vec{\Phi}_n^{(2)} - \frac{i\lambda_n}{\beta_n} \vec{\Phi}_n^{(3)}(\mathbf{x}) \right) e^{i\beta_n x_3}.$$

Thus, we can calculate the most convenient solution of the underdetermined system (C.5), (C.6) and (C.7), corresponding to $a_n^{(3)} = b_n^{(3)}$. This gives $\partial_{x_3} g_n^{j(3)}(0) = 0$. The expression of \vec{G}_j in Lemma 2.2 follows.

REFERENCES

- [1] R. ALONSO AND L. BORCEA, *Electromagnetic wave propagation in random waveguides*, Multiscale Modeling & Simulation, 13 (2015), pp. 847–889.
- [2] T. ARENS, D. GINTIDES, AND A. LECHLEITER, *Direct and inverse medium scattering problems in a planar 3D waveguide*, SIAM J. Appl. Math., 71 (2011), pp. 753–772.
- [3] L. BORCEA AND J. GARNIER, *Paraxial coupling of propagating modes in three-dimensional waveguides with random boundaries*, Multiscale Modeling & Simulation, 12 (2014), pp. 832–878.
- [4] L. BORCEA, L. ISSA, AND C. TSOGKA, *Source localization in random acoustic waveguides*, Multiscale Model. Simul., 8 (2010), pp. 1981–2022.
- [5] L. BOURGEOIS, F. L. LOUËR, AND E. LUNÉVILLE, *On the use of Lamb modes in the linear sampling method for elastic waveguides*, Inverse Problems, 27 (2011), p. 055001.
- [6] L. BOURGEOIS AND E. LUNÉVILLE, *The linear sampling method in a waveguide: a modal formulation*, Inverse Problems, 24 (2008), p. 015018.
- [7] ———, *On the use of sampling methods to identify cracks in acoustic waveguides*, Inverse Problems, 28 (2012), p. 105011.
- [8] ———, *On the use of the linear sampling method to identify cracks in elastic waveguides*, Inverse Problems, 29 (2013), p. 025017.
- [9] S. DEDIU AND J. R. McLAUGHLIN, *Recovering inhomogeneities in a waveguide using eigensystem decomposition*, Inverse Problems, 22 (2006), pp. 1227–1246.
- [10] L. EVANS, *Partial Differential Equations (Graduate Studies in Mathematics vol 19)* (Providence, RI: American Mathematical Society), Oxford University Press, 1998.
- [11] L. ISSA, *Source localization in cluttered acoustic waveguides*, PhD thesis, Rice University, 2010.
- [12] J. D. JACKSON, *Classical electrodynamics*, Wiley New York etc., 2 ed., 1975.
- [13] A. K. JORDAN AND L. S. TAMIL, *Inverse scattering theory for optical waveguides and devices: Synthesis from rational and nonrational reflection coefficients*, Radio Science, 31 (1996), pp. 1863–1876.
- [14] U. KANGRO AND R. NICOLAIDES, *Divergence boundary conditions for vector helmholtz equations with divergence constraints*, ESAIM, Math. Model. Numer. Anal., 33 (1999), pp. 479–492.
- [15] A. KIRSCH, *An integral equation approach and the interior transmission problem for Maxwell’s equations*, Inverse Probl. Imaging, 1 (2007), pp. 159–180.
- [16] W. McLEAN, *Strongly Elliptic Systems and Boundary Integral Operators*, Cambridge University Press, Cambridge, UK, 2000.
- [17] D. W. MILLS AND L. S. TAMIL, *Analysis of planar optical waveguides using scattering data*, J. Opt. Soc. Am. A, 9 (1992), pp. 1769–1778.
- [18] P. MONK, *Finite Element Methods for Maxwell’s Equations*, Oxford Science Publications, Oxford, 2003.
- [19] P. MONK AND V. SELGAS, *Sampling type methods for an inverse waveguide problem*, Inverse Probl. Imaging, 6 (2012), pp. 709–747.
- [20] P. ROUX AND M. FINK, *Time reversal in a waveguide: Study of the temporal and spatial focusing*, J. Acoust. Soc. Am., 107 (2000), pp. 2418–29.
- [21] K. G. SABRA AND D. R. DOWLING, *Blind deconvolution in ocean waveguides using artificial time reversal*, The Journal of the Acoustical Society of America, 116 (2004), pp. 262–271.
- [22] L. S. TAMIL AND A. K. JORDAN, *Spectral inverse scattering theory for inhomogeneous dielectric waveguides and devices*, Proceedings of the IEEE, 79 (1991), pp. 1519–1528.
- [23] C. TSOGKA, D. A. MITSODIS, AND S. PAPADIMITROPOULOS, *Selective imaging of extended reflectors in two-dimensional waveguides*, SIAM Journal on Imaging Sciences, 6 (2013), pp. 2714–2739.
- [24] Y. XU, C. MATAWA, AND W. LIN, *Generalized dual space indicator method for underwater imaging*, Inverse Problems, 16 (2000), pp. 1761–1776.